AD-A064 789 SCIENCE APPLICATIONS INC MCLEAN VA F/G 8/10
RECIRCULATION AND THERMOCLINE PERTURBATIONS FROM OCEAN THERMAL --ETC(U)
1977 S A PIACSEK, P J MARTIN, J TOOMRE N00014-76-C-0610
UNCLASSIFIED NRL-GFD/OTEC 2-76 NL

| OF |
ADA
064789

END
DATE FILMED
4-79
DDC

(18) (19) NRL-GFD/OTEC 2-76

(6) RECIRCULATION AND THERMOCLINE PERTURBATIONS FROM OCEAN THERMAL POWER PLANTS

(19) Steve A. Piacsek, Paul J. Martin, and Juri Toomre
Glyn O. Roberts

Geophysical Simulation Section, Code 7750
Naval Research Laboratory

and

(15) N0001 4-76-C-0610
E(49-26)-1005
Glyn O. Roberts

Fluid Mechanics Division,
Science Applications, Inc.

Supported by the Ocean Thermal Energy Conversion Program, Division of Solar Energy, Energy Research and Development Administration, under ERDA contract E (49-26) 1005 .

RECIRCULATION AND THERMOCLINE PERTURBATIONS FROM OCEAN THERMAL POWER PLANTS.

Steve A. Piacsek, Paul J. Martin and Juri Toomre

Geophysical Simulation Section, Code 7750
Naval Research Laboratory

and

N0014-76-0610

Glyn O. Roberts

Fluid Mechanics Division,
Science Applications, Inc.

Supported by the Ocean Thermal Energy Conversion Program, Division of Solar Energy, Energy Research and Development Administration, under ERDA contract E (49-26) 1005 .

TABLE OF CONTENTS

ABSTRACT

Numerical experiments were performed on the fluid motions resulting from the pumping action of ocean thermal power plants. In particular, the resulting thermocline distortions, sea surface temperature decrease and corresponding heat flow change were investigated. The object was to find engine discharge configurations and pumping rates that would minimize these alterations. This would result in both a minimal environmental impact and preservation of the temperature gradient across the engine, i.e. the energy resource.

The results obtained to date use 2-D turbulent flow calculations. Near the engine, the sea surface temperature reduction ranges from 0.01°F to 3°F, depending on design, flow rate, season and location. The mean temperature of the warm inflow water is reduced by up to 4°F from the mean temperature at that depth, for certain designs and flow rates, due to recirculation and turbulence. The far-field surface heat calculations applied to the Puerto Rico area shows that a depression of the sea surface temperature by 0.1 °C leads to an increased heat flow from air to sea of 9.6 cal/cm^2/day, serving to replenish the heat removed from the surface layers by the plant. Accepting 0.1 °C as a permissible environmental perturbation, the areal requirement for a typical 100 MW plant is 2500 km^2, with a radius of 28 km. The corresponding estimates for Hawaii are 4 cal/cm^2/day, an area of 6000 km^2, and a radius of 44 km.

1. INTRODUCTION

The operation of one or more ocean thermal power plants (OTPP's) in a given geographical region can lead to several geophysical effects. Some of these are: a lowering of ocean surface temperatures; a reduction in the heat content of the surface layers; and an increase in the heat content of the layers below 200 m depth. A severe modification of the thermal structure near the plant could result in a lower temperature contrast across the plant, and thus reducing the thermal resource available for power extraction. Furthermore, horizontal ocean currents and turbulence can disperse the perturbations to considerable distances beyond the region of operation, and the area-integrated cumulative effect may cause a slight alteration in the regional climate. It is important to demonstrate that the areal extent and magnitude of any alteration is within acceptable limits.

2. TURBULENT FLOW NEAR THE PLANT

The first problem that must be solved before any of the above environmental impact questions can be tackled is the "exterior fluid dynamics" of the plant, i.e. the fluid motions directly forced by the engine pumps. The basic hydrodynamic flow problem associated with an OTPP is that of source-sink flows in a stratified fluid. The source-sink flows between the warm and cold intakes and between the warm and cold discharges are not a potential flow, i.e. irrotational, because the horizontal buoyancy variations in a stratified fluid produce rotation. The exact nature of the resultant flow is determined by the relative strengths of the pumping action and the ocean's stratification. The relevant non-dimensional hydrodynamic parameter governing high Reynolds number source-sink

flow in a stratified fluid is the Froude number, defined as

$$Fr = U/DN$$

where U is the discharge velocity, D is the diameter of the discharge pipe and $N = (g/\rho_o)^{\frac{1}{2}} (d\rho/dz)^{\frac{1}{2}}$ is the Brunt-Vaisala frequency of buoyancy motions in the respective thermocline.

The primary effect of the turbulent eddies is to diffuse momentum, heat and salt, much as molecular diffusivity with a large value does (the effective diffusivity of wind-generated turbulence in the ocean is $\sim 10^2$ cm^2/sec). Unfortunately, a direct simulation of the turbulent eddies of all sizes is not feasible on present-day computers with a storage of the order of 10^6 words. Thus recourse must be made to some kind of closure method where the effects of the small eddies are represented as turbulent transport terms in the mean flow equations.

A first-order statistical closure model is adopted for modelling the turbulent flow in these studies. The flow variables are split into the ensemble mean and a perturbation, and only statistical average products are calculated for the perturbation parts (Mellor and Yamada[1], Lewellen [2,3]). In the mean flow equations the turbulence transport terms are determined from the divergence of fluxes that are the products of an eddy diffusion coefficient and mean flow gradients. The model equations are presented in Table 1.

A single turbulent diffusivity K is used in equations (1), (2) and (3) for the diffusion of momentum, temperature and turbulence kinetic energy $q = \frac{1}{2} \overline{u_i' u_i'}$ in both the horizontal and vertical directions. In this simple model, K is calculated from q and a length scale L, the integral length scale of turbulence, as $K = L\, q^{\frac{1}{2}}$, with L being an imposed constant.

TABLE 1.

EQUATIONS TO IMPLEMENT THE TURBULENCE MODEL

The momentum equations are represented by

$$\frac{Du_i}{Dt} = -\frac{\partial P}{\partial x_i} + \frac{\partial}{\partial x_j}\left\{ K\left(\frac{\partial u_i}{\partial x_j} + \frac{\partial u_j}{\partial x_i}\right)\right\} + \left(T - C_w \frac{K N^2}{q} u_3\right)\delta_{i3} , \quad (1)$$

the heat equation by

$$\frac{DT}{Dt} = \frac{\partial}{\partial x_j}\left(K \frac{\partial T}{\partial x_j}\right) , \quad (2)$$

the turbulence equation by

$$\frac{Dq}{Dt} = K\left\{\frac{1}{2}\left(\frac{\partial u_i}{\partial x_j} + \frac{\partial u_j}{\partial x_i}\right)^2 - N^2 + C_w \frac{N^2 u_3^2}{q}\right\} - C_f \frac{K q}{L^2} + \frac{\partial}{\partial x_j}\left(K \frac{\partial q}{\partial x_j}\right) , \quad (3)$$

and continuity by

$$\frac{\partial u_i}{\partial x_i} = 0 , \quad (4)$$

where

$$\frac{D}{Dt} \equiv \frac{\partial}{\partial t} + u_j \frac{\partial}{\partial x_j} , \quad N^2 = \frac{\partial T}{\partial x_3} , \quad (u_1, u_2, u_3) \equiv (u, v, w) ,$$

$$K = L\, q^{1/2} \left(1 + C_s N^2 L^2 / q\right)^{-1} . \quad (5)$$

Usually the parameters are chosen as

L = 0.3 × (depth of region) , $C_f = 2$, $C_s = 0.1$, and $C_w = 0.1$.

Here K is modified by the factor $(1 + C_s N^2 L^2/q)^{-1}$ in (5), representing the suppression of vertical turbulent transports when q is small compared with N^2L^2. As presented in Table 1, the model has three arbitrary constants to be determined. Unfortunately, these constants are not universal but have to be changed for each physical situation, and are usually obtained from experiments.

The first term on the right-hand side of (3) represents production of turbulence by the mean flow gradients. The second term represents loss of turbulence energy through turbulent entrainment of different density layers, which appears in the vertical diffusion term in (2) as increase in potential energy. With negligible mean flow, q becomes zero in a finite time if $C_s = 0$ in (5). The fourth term controls the self-decay of turbulence through a cascade to very small length scales where molecular viscosity is important.

In order to prevent the turbulence from decaying in a finite time to zero according to the relation $dq/dt \sim - Lq^{\frac{1}{2}} N^2$, the usual relation $K = L q^{\frac{1}{2}}$ has been replaced by the form given in (5) of Table 1. Then in regions of strong stratification the relation $dq/dt \sim -c_s q^{3/2}$ will hold and the decay of turbulence will slow down. This can also be looked upon as the inclusion into the shear-produced turbulence energy density of the small-scale, random internal waves generated in these regions.

The term $- c_w K N^2 w/q$ in the w equation is included to suppress the instability of the mean flow, and to represent the loss of energy from the mean flow to random internal waves. There is a corresponding term in equation (3). The second term on the right-hand side of (1) represents the viscous effect of the turbulent eddies on the mean flow.

A series of experiments was run to test the effect of the Froude number on the nature of the flow. The experiments were kept simple by introducing linear stratification, so that only the top half of the

discharge jet and the bottom half of the intake flow needed to be included. The resultant streamlines are displayed in Figure 1 . They show that for Fr = 3.2 (Fig. 1a) only 10% of the discharge flow exits through the right-hand boundary. For Fr = 1.6 (Fig. 1b) the corresponding figure is 55% , and for Fr = .80 (Fig. 1c) the outflow is over 100% , i.e. some flow is actually entrained from infinity and goes back without ever reaching the left wall. The above series was run with the constants listed in Table 1 and with orifice radii a quarter of their separation.

The next series of experiments was designed to simulate a more realistic OTPP configuration. The source-sink flow consisted of a warm water intake and a discharge below it that ejected either the ingested water cooled by $3^{o}F$ or cold water at $50^{o}F$. The latter case represents a discharge of the cold bottom water over the warm discharge, as suggested by TRW[1]. The depth of the simulation volume is 100 m, and the top represents the water surface. The intake is at 20 m below the surface, and the discharge at 50 m. The temperature at the bottom is $T_{100} = 69^{o}F$ and at the surface $T_s = 85^{o}F$. A realistic thermocline of the analytic form

$$T(z) = A + B \tan^{-1} [(z - z_c)/\delta]$$

was used, where A and B are constants such that $T_{z=100}$ and T_s have the prescribed values. The center or point of inflection of the thermocline is at $z_c = 50$ m depth, and its "width" is 50 m. This corresponds to a typical August thermocline in the Gulf of Mexico.

Figure 2 depicts the resulting thermocline deformations for a warm (cooled by $3^{o}F$) and a cold ($50^{o}F$) discharge, respectively. The approximately $4^{o}F$ temperature drop at the intake depth in the case of the warm discharge indicates a reduction of 10% for the temperature contrast

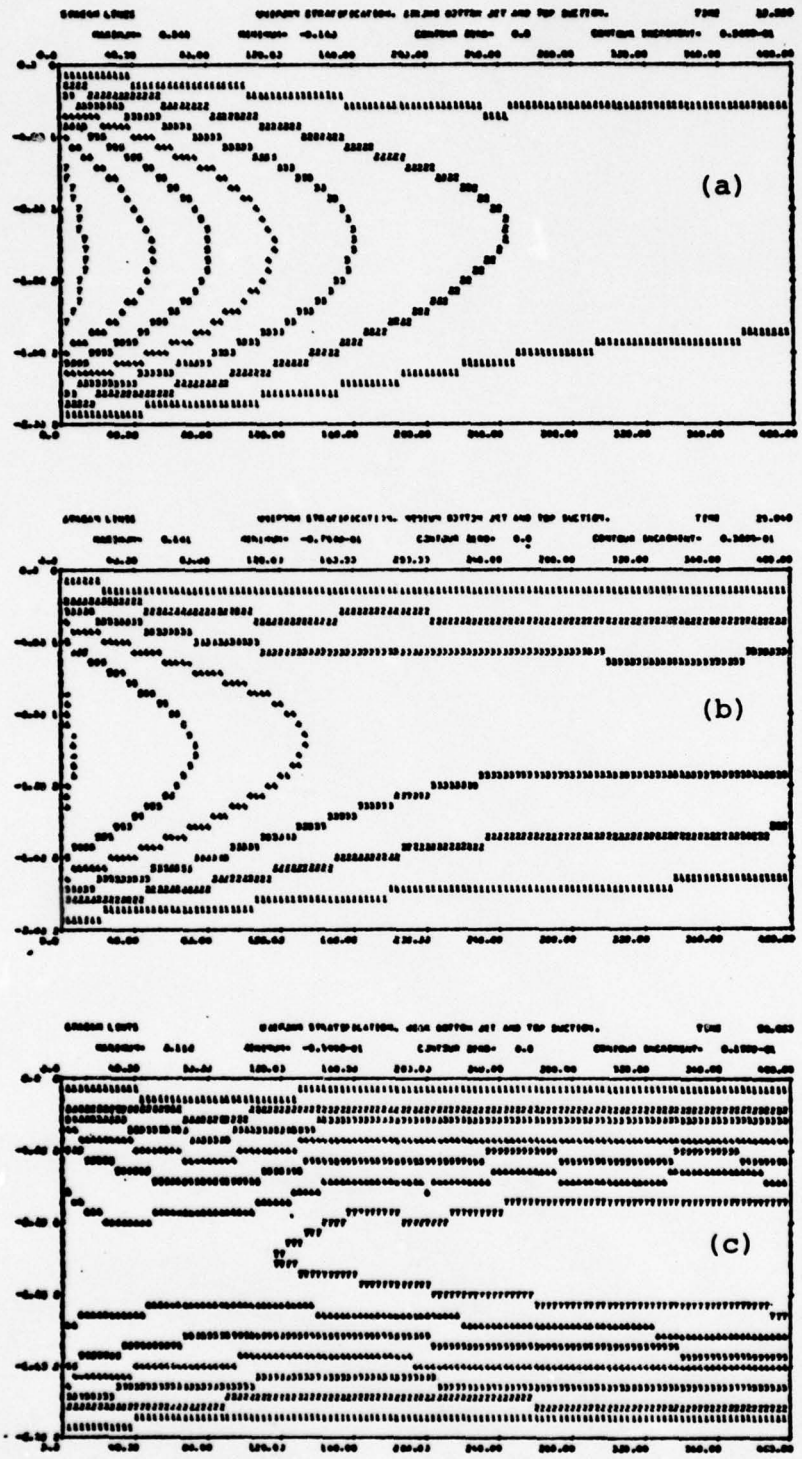

Figure 1. Streamlines for steady 2-D flows obtained with idealized sink (left top) and source (left bottom) driving. The computational domain is a vertical cross-section 200 ft in depth and 400 ft in horizontal extent. The three cases illustrate the effects of increasing the stratification strength, with corresponding Froude numbers Fr = 3.2 (a), Fr = 1.6 (b), and Fr = 0.8 (c).

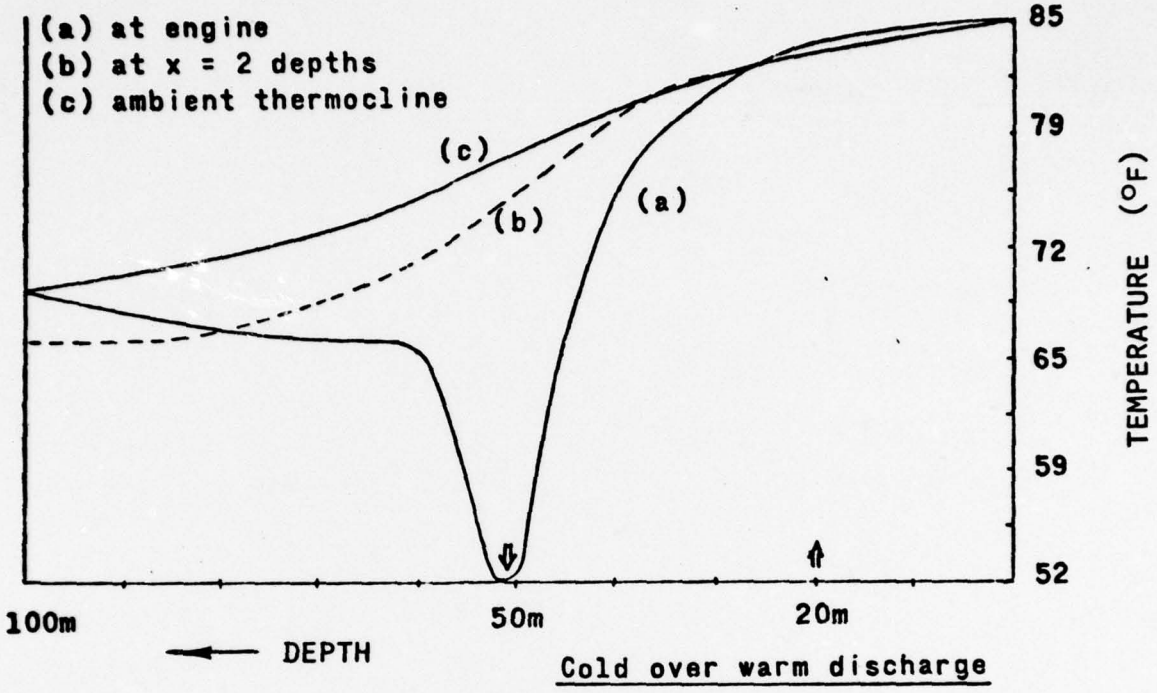

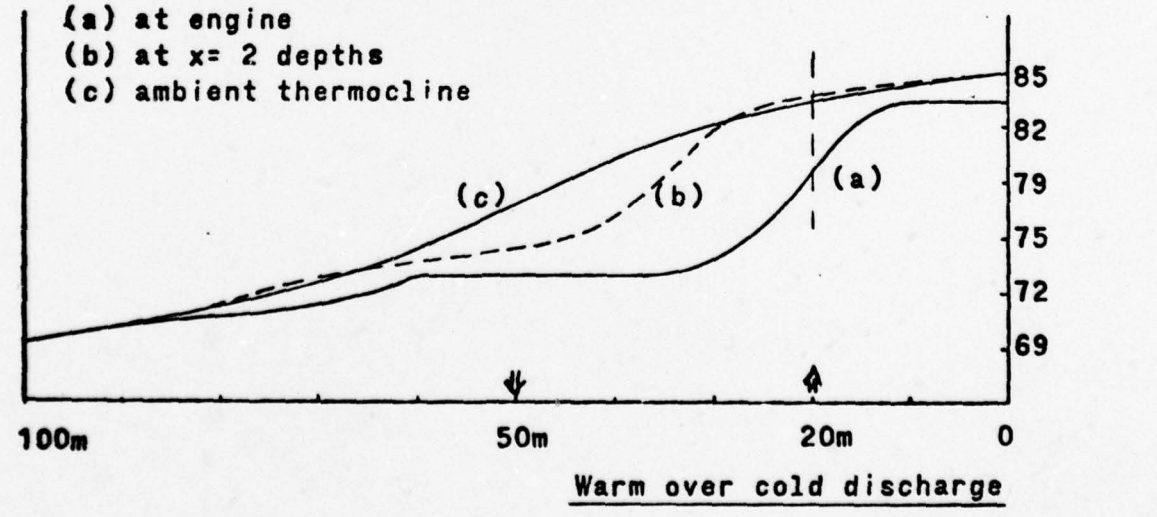

Figure 2. Thermocline deformations as a function of discharge configuration and horizontal distance from the power plant. The stratification is typical of the Gulf of Mexico in August.

across the engine. On the other hand, in the case of the cold discharge there is no temperature loss at the intake level, but there is an anomalously cold region of considerable width between the 50 m and the 100 m depth levels that has a horizontal extent of several kilometers. As a result, the surface temperature is lowered over a wider area and to a lower value in the case of the cold discharge over the warm discharge. Figure 3 shows the corresponding streamlines of these "two-hole" experiments, for a Froude number of Fr = 4. In the case of the warm discharge (Fig. 3a) approximately half the flow recirculates, and about 10% is entrained to and from infinity. In the case of the cold discharge there is no recirculation but ~40% is entrained to and from infinity.

Finally, a series of "three-hole" experiments was run with both warm and cold discharges present. The geometry consisted of a 2-D equivalent of the Lockheed baseline design, with the flow rates determined as if the inlet and outlet ports were effectively 75 ft high and 100 ft wide. The thermocline used corresponds to that of the Gulf of Mexico in August, and the Froude number based on a slit height and N at the cold water discharge depth is Fr = 1.8. The total depth of the simulation volume was 500 ft, the intake depth 50 ft and the depths of the warm and cold water discharges 150 ft and 300 ft, respectively. Figure 4 illustrates the streamlines for this design. Each contour increment represents a flux of 2000 ft^3/sec of water; the total warm water circulation is 15% less than the total cold water circulation. There is an ~16% recirculation between intake and warm discharge, and approximately 50% of the "warm" discharge (3^oF below intake temperature) sinks rapidly to join the cold discharge in a distance less than 100 ft from the plant.

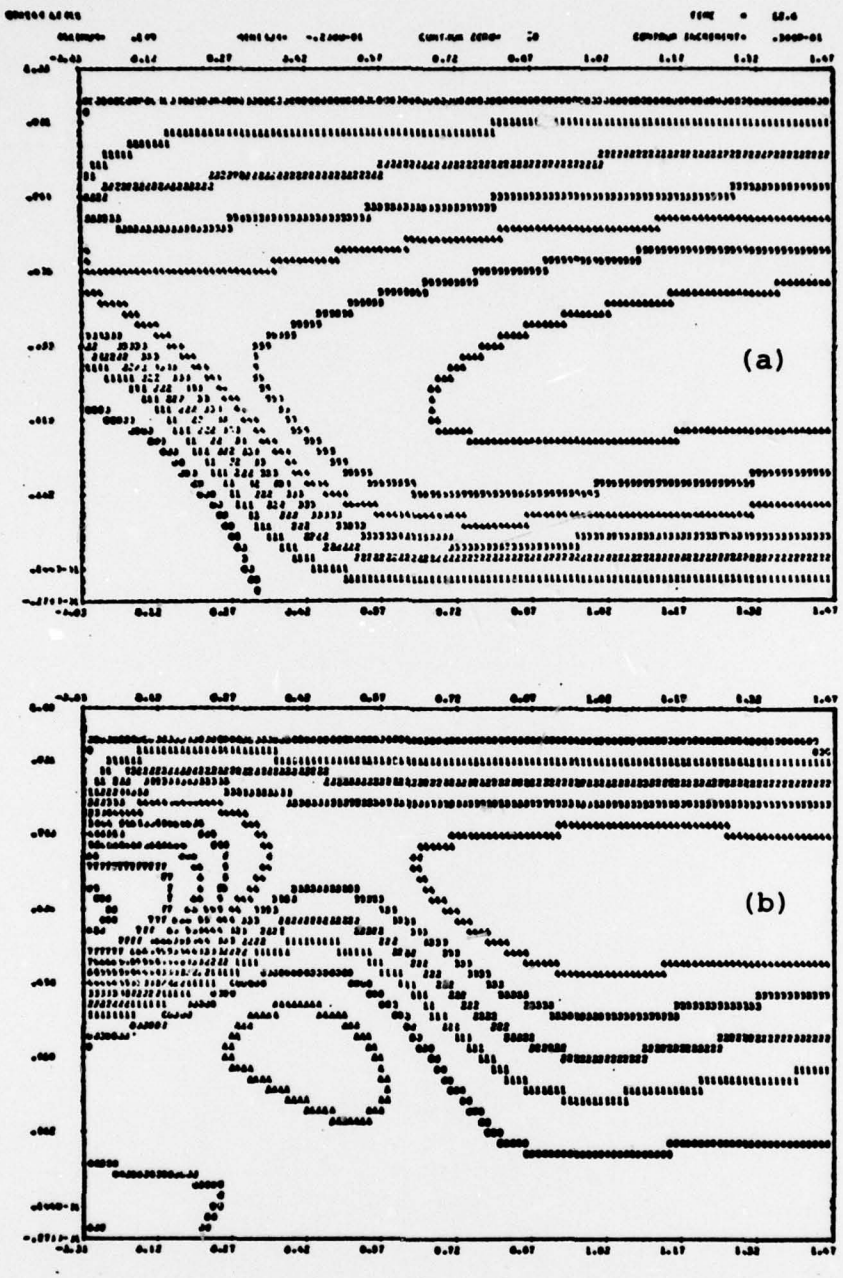

Figure 3. Streamlines for 2-D flow designed to simulate circulation between intake near surface and discharge at depth, for two different realizations. Flow parameters represent early TRW design values. In case (a), the discharge water temperature is fixed at 50°F, representing condenser outflow. In case (b), the discharge water is 3°F cooler than intake, and models evaporator outflow. The stratification is typical of the Gulf of Mexico in August. The portion of the computational domain shown is a vertical cross-section 100 m in depth and 150 m in horizontal extent.

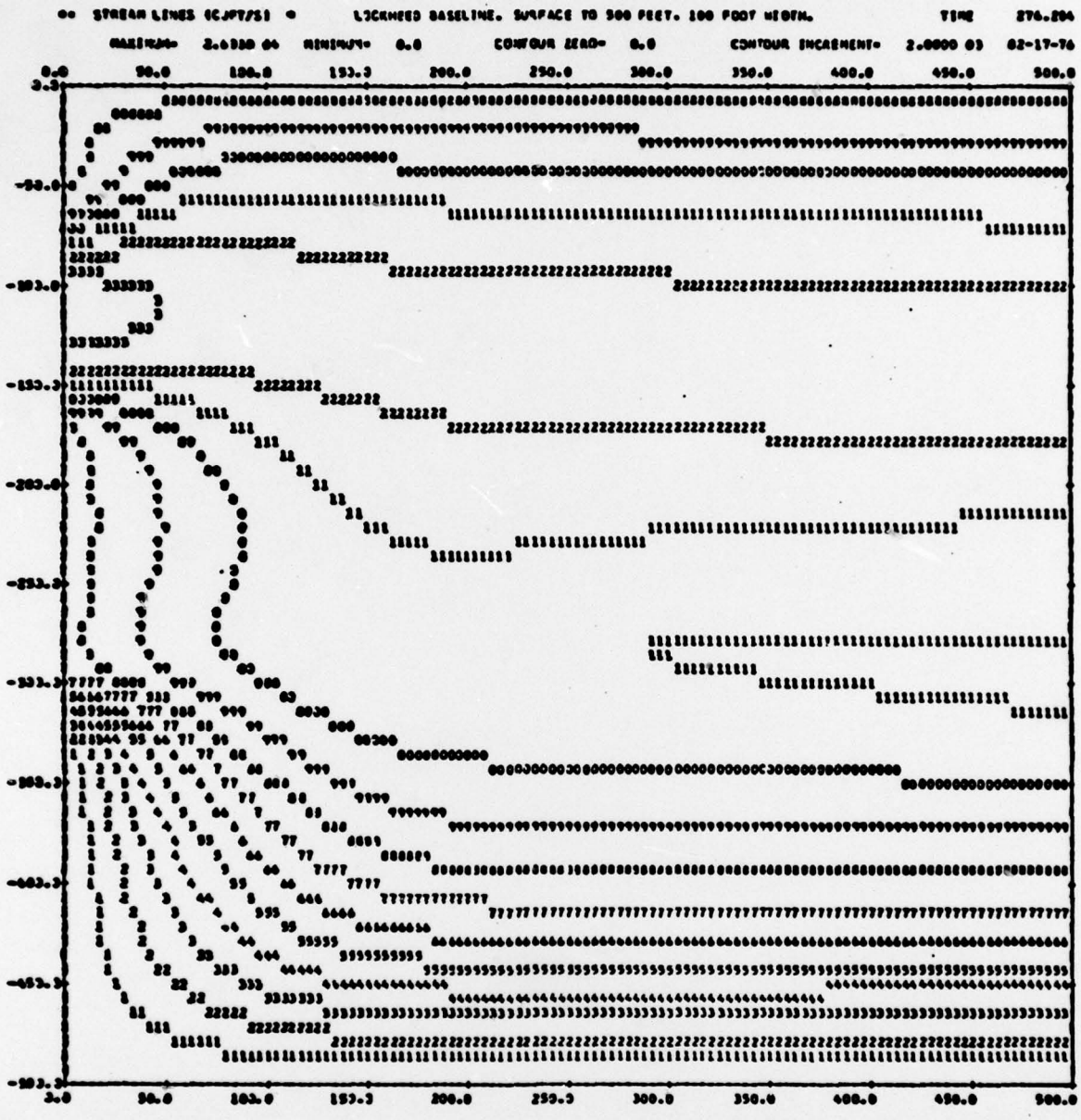

Figure 4. Streamlines for steady 2-D flow designed to simulate a Lockheed baseline plant. The portion of the computational domain shown is a vertical cross-section 500 ft in depth and 500 ft in horizontal extent. The intake is at 50 ft depth and the warm and cold discharge are located at 150 and 300 ft . The inflow and outflow ports each occupy 75 ft in the vertical. The density profile is typical of the Gulf of Mexico in August.

3. SEA SURFACE TEMPERATURE (SST) DEPRESSION

A series of "three-hole" experiments was performed on various thermoclines for regions[11] east and southeast of the United States, for the months of August and February. Tables 2 and 3 present the relevant ocean temperature information and results for the case of Fr = .5, with warm over cold discharge configuration (inflow at 25m, outflow at 50m, radii 5m) in the month of August. The temperature differences between the surface and the 100m depth (dT(100m)) represent the relative strength of the stratifications in the depth region where most designs plan to discharge the warm and cold water. The temperature differences between surface and the 500m depth (dT(500m)) represent the available thermal resource.

Table 3 summarizes the resultant sea surface temperature lowerings, dT_s, for various designs and Froude number ranges; the average values of dT_s over the indicated Froude number range is given. In general, dT_s is a function of the discharge configuration (warm over cold, etc.), the cold water discharge temperature, and the stratification present in the top 100m of the ocean. The cold over warm discharge configuration results in a consistently larger SST depression for both Froude number ranges. Typically, in the range $.5 \leq Fr \leq 1.5$ the SST depression is $\sim .25^{\circ}F$ in August and $\sim .08^{\circ}F$ in February, whereas in the range $2 \leq Fr \leq 8$ the cooling is $\sim 2^{\circ}F$ in August and $\sim .50^{\circ}F$ in February. Again, the larger stratifications in August result in larger SST depressions than in February. Finally, the large SST depressions associated with the high Froude number range are due to the stronger recirculation and stronger turbulence intensity produced by the increased source-sink flow.

TABLE 2.

OCEAN THERMAL RESOURCE SURVEY

Region	dT(100m)	dT(500m)	Location
1	21	34	West of Africa, 5^{o}-15^{o} latitude
2	16	33	Equatorial Atlantic
3	7	29	Caribbean and eastward
4	5	29	Eastern Gulf, Cuba - Florida Straits
5	16	39	Gulf of Mexico
6	11	17	East of Gulf Str. (Fla. - S.C. latitude)
7	9	29	Gulf Stream
8	20	37	Gulf Stream - Shore
41	9	21	West of Africa, 10^{o}-30^{o} latitude

Geographical distribution of thermal structure in the upper 500 m of the oceans, in the month of August. The definition and location of the regions is given in the Oceanographic Atlas[11]. The temperature ^{o}F difference between the surface and 100 m depth is denoted by dT(100m) and represents the strength of the stratification in the depth range where most plant designs plan to discharge both the warm and the cold water. The temperature difference in ^{o}F between surface and 500 m depth is denoted by dT(500m) and represents the available thermal resource.

TABLE 3.

Maximum surface temperature perturbation near the plant (in ^{o}F) for the idealized plant configuration in Figure 3.

Design		1	2	3	4
Caribbean and East	Aug	.12	.11	.92	.64
	Feb	.051	.045	.39	.28
Gulf of Mexico	Aug	.27	.24	2.10	1.48
	Feb	.085	.075	.66	.46
Gulf Stream to Shore	Aug	.34	.30	2.62	1.84
	Feb	.10	.09	.79	.55

Design 1: cold over warm discharge, low Froude number $.5 \leq Fr \leq 1.5$

Design 2: warm over cold discharge, low Froude number "

Design 3: cold over warm discharge, high Froude number $2.0 \leq Fr \leq 8.0$

Design 4: warm over cold discharge, high Froude number "

4. AIR-SEA HEAT FLUX PERTURBATIONS

The operation of one or more OTPP's in a given geographical region has been shown to produce a reduction in ocean surface temperatures in that region. It has been observed experimentally, and is predictable from theoretical calculations, that a lowering of the sea surface temperature generally leads to an increased heat flow from air into the water. This is because the process most susceptible to change, evaporation, responds to a sea surface temperature lowering by decreasing the heat flux from the water to the air. It is important to note that the far-field rate of recovery of the ocean toward its undisturbed thermal structure is determined by the area and magnitude of sea surface temperature lowering.

An OTPP extracts heat at a rate $\simeq$ 50 times its power output (2% efficiency) from the warm surface water passing through its evaporators. Unless the ocean replenishes the extracted heat at a sufficiently rapid rate over the area affected by the intake motions, the available temperature contrast and thermal resource entering the plant will be continuously reduced, at least in the absence of a current. Furthermore, the impact of the engine on the surface temperatures and the marine atmospheric boundary layer will continuously grow. In this study we performed specific heat flux perturbations due to SST depressions caused by OTPP operations. The sea surface temperature perturbations were taken from the result of the near-field hydrodynamic calculations. By calculating the integrated heat-flux effect over the whole area affected by the intake motions, an estimate has been made for the areal requirement for thermal resource of an OTPP.

Because both the latent heat flux and the sensible heat flux depend upon the air-sea temperature difference, the sea surface temperature acts as a feedback mechanism for regulating the heat budget of the upper ocean.

Neglecting the storage of heat in the upper ocean due to seasonal temperature variations which are small in the tropical regions being considered for OTPP operation, the sea surface temperature tends to be maintained at a value such that the heat gained by the absorption of solar radiation minus the heat lost to the atmosphere just balances the heat carried away by horizontal advection and diffusion. If, for example, more heat is added to the upper ocean than is being carried away by advection and diffusion, the sea surface temperature increases, increasing the rate of heat loss to the atmosphere which in turn drives the sea surface temperature back towards its equilibrium value.

The tendency of the sea surface to maintain a certain temperature is observed in the recovery of the upper ocean from the disruptive effects of storms and hurricanes which can lower the sea surface temperature several degrees due to upwelling, evaporation, and downward mixing. For example, Leipper[6] noted that in the Gulf of Mexico surface temperature had returned to normal within two months after hurricane Hilda had lowered sea surface temperatures up to 5°C.

The speed with which the sea surface temperature returns to its equilibrium value after being perturbed depends upon the rate of change of the sea surface heat flux with sea surface temperature, dQ/dT_s. Bathen[7], using bulk aerodynamic formulas and local meteorological data, analysed the oceanic heat budget off Keahole Point, Hawaii, a proposed OTPP site, and determined that if the sea surface temperature decreased 0.67 °C due to OTPP operation, the loss of heat to the atmosphere would decrease 40-50 cal/cm^2/day. Therefore, the rate of change of sea surface heat flux with sea surface temperature was determined to be about 60-70 cal/cm^2/day/°C.

Although we were unable to repeat Bathen's calculations due to the unavailability of the necessary meteorological data, a similar prediction of the change of the surface heat flux with sea surface temperature was

made for a proposed site off the southeast coast of Puerto Rico at 17.5°N, 67.5°W using bulk formulas detailed by Laevastu[8] and Wyrtki[10], and meteorological data from Atwood[9]. The surface heat fluxes determined using the observed sea surface temperatures near Puerto Rico are listed in Table 4. The heat fluxes in Table 4 were calculated for each month and the monthly values were averaged to obtain the yearly mean.

Due to the crude state of the art of estimating sea surface heat fluxes using bulk formulas, the estimates of the sea surface heat fluxes in Table 4 must be regarded as fairly rough approximations. For example, published estimates of the drag coefficient for latent heat loss have a variation of $\pm$ 20 %. Therefore, allowing for an uncertainty of 15% in the windspeed and humidity values, the uncertainty of the latent heat loss is about 30%, and the uncertainty of the sensible heat loss, which was calculated from the latent heat loss using a Bowen ratio of 0.1, is probably 40% or more.

In order to obtain an estimate of the change in the net sea surface heat flux that might occur near Puerto Rico due to a local drop in the mean sea surface temperature, the surface heat fluxes near Puerto Rico were recalculated using sea surface temperatures reduced by 0.5 °C and 1.0 °C from the observed values and the results are summarized in Table 5. In determining the heat fluxes it was assumed that the air temperature well above the sea surface was not significantly affected by the local change in the sea surface temperature. Table 5 shows that the rate of change of the surface heat flux with sea surface temperature is about 96 cal/cm^2/day/°C. The change in the net sea surface heat flux with sea surface temperature is fairly linear because, for changes in sea surface temperature of less than a few degrees centigrade, the back radiation

TABLE 4.

RTO RICO DATA. ALL AVE VALUES ARE AVERAGED OVER THE 12 MONTHS.

SURFACE TEMPERATURE LOWERED 0.0 DEG C FROM OBSERVED VALUE

	JAN	FEB	MAR	APR	MAY	JUN	JUL	AUG	SEP	OCT	NOV	DEC	AVE
N SUN ANGLE (DEG)	49.	57.	69.	79.	89.	93.	91.	84.	72.	62.	52.	47.	70.
GTH OF DAY (MIN)	672.	695.	721.	757.	778.	790.	785.	764.	734.	705.	679.	665.	729.
N CLOUDINESS IN TENTHS	0.33	0.34	0.30	0.36	0.41	0.43	0.42	0.32	0.37	0.36	0.37	0.34	0.36
TEMP IN DEG C	25.0	25.0	25.0	25.6	26.7	27.2	27.2	27.8	27.8	27.2	27.2	25.6	26.4
ER TEMP IN DEG C	25.6	25.6	25.6	26.1	27.2	27.8	27.8	28.3	28.3	28.3	27.8	26.7	27.1
PRESS IN MB	1018.	1018.	1017.	1017.	1017.	1017.	1018.	1017.	1016.	1016.	1017.	1017.	1017.
N WIND CM/SEC	885.	885.	885.	740.	740.	740.	735.	735.	735.	730.	730.	730.	772.
OR PRESS MB	24.504	24.504	24.507	25.349	27.130	28.068	28.069	29.038	29.036	28.067	28.069	25.349	26.808
CIFIC HUMIDITY AIR	0.01511	0.01511	0.01513	0.01565	0.01676	0.01735	0.01733	0.01795	0.01797	0.01736	0.01735	0.01565	0.01656
CIFIC HUMIDITY SURF	0.02034	0.02034	0.02036	0.02107	0.02256	0.02334	0.02332	0.02415	0.02417	0.02417	0.02334	0.02180	0.02241
IDENT RADIATION	425.	512.	646.	728.	732.	731.	730.	748.	671.	556.	448.	404.	611.
FLECTED RADIATION	-46.	-51.	-55.	-56.	-56.	-56.	-56.	-56.	-56.	-52.	-47.	-44.	-53.
SOLAR RADIATION	379.	461.	591.	672.	676.	675.	674.	692.	615.	503.	401.	360.	558.
K RADIATION	-126.	-126.	-128.	-122.	-115.	-111.	-111.	-112.	-111.	-122.	-114.	-131.	-119.
PORATIVE HEAT LOSS	-340.	-340.	-341.	-294.	-315.	-325.	-323.	-334.	-334.	-364.	-321.	-329.	-330.
SIBLE HEAT LOSS	-34.	-34.	-34.	-29.	-31.	-33.	-32.	-33.	-33.	-36.	-32.	-33.	-33.
HEATING OF OCEAN	-121.	-39.	88.	226.	215.	206.	208.	212.	137.	-19.	-66.	-134.	76.

An estimate of the sea surface heat fluxes for the ocean thermal power plant site SE of Puerto Rico. The heat fluxes were calculated for each month and the monthly values were averaged to obtain the yearly mean values. The heat fluxes are in units of cal/cm^2/day.

TABLE 5.

Decrease of T_s from ambient value	0° C	0.5° C	1.0° C
Net solar radiation	558	558	558
Back radiation	-119	-112	-105
Latent heat loss	-330	-292	-255
Sensible heat loss	-33	-29	-26
Net surface heat flux	76	125	172

Surface heat flux variation with sea surface temperature at proposed Puerto Rico OTPP site, in units of cal/cm^2/day. Positive flux represents heat flow from air into water.

and the latent and sensible heat fluxes vary almost linearly with sea surface temperature.

Most of the change in the sea surface heat flux due to the decrease in the sea surface temperature, almost 80%, is due to the decrease in the evaporative heat loss. And if the Bowen ratio R is used to estimate the sensible heat loss, the bulk formula for latent heat loss effectively models about 85% of the change in surface heat flux with sea surface temperature.

ACKNOWLEDGMENTS

Portions of this report were presented at the symposium on "Energy from the Oceans --- Fact or Fantasy?" held at North Carolina State University on 27-29 January 1976. The research work described here was supported by the Ocean Thermal Energy Conversion Program, Division of Solar Energy, Energy Research and Development Administration, under ERDA contract E (49-26) 1005 .

REFERENCES

1. Mellor, G. L., Yamada, T. "A Hierarchy of Turbulence closure Models for Planetary Boundary Layers", J. Atmos. Sci. 31, p 1791, 1974.
2. Lewellen, W. S., Teske, M. "Prediction of the Monin-Obukhov Similarity Functions from an Invariant Model of Turbulence", J. Atmos. Sci. 30, p. 1340, 1973.
3. Lewellen, W. S. et al. "Invariant Modeling of Turbulence and Diffusion in the Planetary Boundary Layer", ARAP Rep. 225, Aeronautical Research Associates of Princeton, N. J., 1974.
4. Douglass, R. et al. "Ocean Thermal Energy Conversion: An Engineering Evaluation". Third Annual OTEC Workshop Proc., Houston, May 1975.
5. Trimble, L. et al. Third Annual OTEC Workshop Proc., Houston, May 1975.
6. Leipper, D. F. "Observed Ocean Conditions and Hurricane Hilda", J. Atmos. Sci. 24, p. 182, 1967.
7. Bathen, K. H. et al. "A further evaluation of the oceanographic conditions found off Keahole Point, Hawaii, and the environmental impact of nearshore OTEC plants on subtropical Hawaiian waters. Final report, Dep't of Ocean Engin., Univ. of Hawaii.
8. Laevastu, T., "Factors affecting the temperature of the surface layer of the sea". Soc. Scient. Fennica, Comm. Phys. Mat. 25, p.1, 1960.
9. Atwood, K. K. et al. "Ocean Thermal Energy Conversion: Resource Assessment and Environmental Impact for Proposed Puerto Rico Site. Interim Report, NSF Grant No. AER 75-00145, Dep't of Marine Sciences, Univ. of Puerto Rico, Mayaguez.

10. Wyrtki, K. "Seasonal Variation of Heat Exchange and Surface Temperature in the North Pacific Ocean. Report No. 66-3, Hawaii Institute of Geophysics, University of Hawaii.

11. "Oceanographic Atlas of the North Atlantic Ocean", Section II, Physical Properties. Publ. No. 700, U.S. Naval Oceanographic Office, Washington, D.C. 1967.